Short-circuit Analysis in Large-scale Distribution Systems With High Penetration of Distributed Generators

Luka V. Strezoski, *Student Member, IEEE*, and Marija D. Prica, *Member, IEEE*

***Abstract*—In this paper a short-circuit computation (SCC) procedure for large-scale distribution systems with high penetration of distributed generators based on contemporary technologies is proposed. The procedure is suitable for real-time calculations. Modeling of modern distributed generators differs from the modeling of traditional synchronous and induction generators. Hence, SCC procedures found on the presumption of distribution systems with only traditional generators are not suitable in nowadays systems. In the work presented in this paper, for computation of the state of the system with short-circuit, the improved backward/forward sweep (IBFS) procedure is used. Computation results show that the IBFS procedure is much more robust than previous SCC procedures, as it takes into account all distribution system elements, including modern distributed generators.**

***Index Terms*—Distributed generation (DG), distribution system, distribution management system (DMS), short-circuit computation.**

I. Introduction

IN In the past, electrical energy was produced in bulk by large power plants and transmitted to the high voltage/medium voltage (HV/MV) substations. Each of the substations was a single supply point of the respective distribution system. Distribution systems consisted of passive elements such as line sections, transformers, capacitor banks, etc. and no energy was produced there. Power flow was from the HV/MV substation to the consumers. Similarly, the fault-current flow was from the HV/MV substation to the fault location.

Nowadays, this situation is rapidly changing. In the last few decades the number of distributed generators (DGs) is rapidly growing around the globe. The reason behind this is that DGs provide many benefits to the distribution system operation. Some of these benefits are: energy losses could be decreased, DGs could contribute with a reactive power support, DGs could contribute in preserving stable voltage profile along the feeders, and most importantly, DGs are largely from "green" energy resources, such as wind and sun, and thus they could help in the combat with nowadays energy and environmental issues.

Manuscript received March 5, 2016; accepted June 22, 2016. Recommended by Associate Editor Xiangyang Zhao.

Citation: L. V. Strezoski and M. D. Prica, "Short-circuit analysis in large-scale distribution systems with high penetration of distributed generators," *IEEE/CAA Journal of Automatica Sinica*, vol. 4, no. 2, pp. 243−251, Apr. 2017.

L. V. Strezoski and M. D. Prica are with the Case School of Engineering, Case Western Reserve University, Cleveland 44106, Ohio, USA (e-mail: lxs533@case.edu; mxp438@case.edu).

Digital Object Identifier 10.1109/JAS.2017.7510517

Nonetheless, it is generally known that integrating large amount of DGs is accompanied with several serious challenges. Nowadays distribution systems are not passive anymore. They are rather active, as a consequence of installed DGs. Thus, power and fault-current flows are no more straightforward. Additionally, a huge share of contemporary DGs' models differs from the traditional generators' models. Accordingly, DGs obviously complicate the operation and management of distribution systems. Thus, classical calculations, based on the presumption of distribution systems with just synchronous or induction machines, cannot be used in nowadays systems.

In an effort to oppose the challenges of the contemporary technologies, the distribution management system (DMS) has become a highly attractive software package. DMS consists of broad selection of power calculations constructed to monitor, control and plan the whole distribution system smoothly and accurately. Short-circuit computation (SCC) is one of the most important DMS power calculations. Results obtained by SCC are mandatory for execution of many different DMS power calculations, such as: relay protection settings and coordination, short-circuit location, isolation and supply restoration, fault management and numerous other calculations. They are also used for protection equipments election, bus-bars construction, etc. The full spectrum of the short-circuit currents results attained by real-time SCC is used to afford safety and differentiation of the whole protection system. Thus, the real-time SCC needs to satisfy two necessary assets: it needs to be fast, and it needs to be highly accurate.

A distribution system SCC procedure is proposed in the International IEC 60909 Standard [1]. This procedure is known as equivalent voltage source (EVS), but as it is presented in [2], EVS is not usable in nowadays distribution systems which contain contemporary DGs. DGs which are built on doubly-fed induction generators (DFIGs) and inverter based DGs (IBDGs) present special challenges. In [2], an extensive table of DGs based on different technologies is shown. Moreover, an attempt to expand the EVS method in order to deal with modern DGs is suggested. However, just symmetrical three-line-to ground faults were considered in [2], but as unsymmetrical faults are prevalent in everyday-life, a SCC needs to handle these types of faults also. In [3], [4] a hybrid compensation method (HCM) is proposed for SCC of large-scale distribution systems. The HCM uses a compensation procedure for calculating the currents in loops, short-circuit currents, and currents of synchronous generators. Subsequently, backward/forward sweep (BFS) in three-phase domain computes the state of the system with short-circuit. BFS is branch oriented method, so it does not depend upon inversion or factorization of the (huge) admittance matrix. This feature makes the HCM particularly fast and efficient for distribution systems with large number of buses. Nonetheless, HCM is built on a presumption that synchronous machines are the lone active parts in the system, and therefore it is not useful for SCCs in distribution systems that contain modern DGs. A more up-to-date SCC method for distribution systems is proposed in [5]. That method is executed in the sequence domain, and it is presented that the sequence domain approach is up to three times faster than the three-phase approach. The limitation of that method is that DGs were not discussed at all. Moreover, [5] is based on building and factorization of the (huge) admittance matrix. Although the admittance matrix approach is exceptionally efficient for transmission systems, it is presented in [6] that it is up to three times slower than the BFS for modeling and calculation of large distribution systems.

The method proposed in this work is built on the superposition theorem [7], [8]. For calculation of the faulted system state, an improved BFS procedure (IBFS) is proposed. The IBFS does not depend on building and inversion (factorization) of the admittance matrix, and it is executed in the sequence domain. Thus, the three phase system is scaled down to three single-phase systems, for positive, negative and zero sequence. These features make the SCC method proposed in this paper fast and simple for calculation. All of the contemporary DG technologies are taken into account and modeled with the up-to-date models [9]−[16]. DFIGs and IBDGs are particularly stressed because their models cannot be integrated into the traditional SCC methods. A decision-making algorithm for determining which model is appropriate, depending on the location of the short-circuit, DFIG's parameters and control settings is proposed in this paper. Moreover, low voltage ride through (LVRT) requirements regarding DFIGs and IBDGs are considered in the algorithm. Loop currents and currents supplied by DGs are computed simultaneously with the whole distribution system state using the proposed IBFS method. Thus, unlike methods proposed in [3], [4], IBFS does not requirean additional iterative procedure.

The SCC method proposed in this paper (IBFS) is compared with the EVS method [1]. The computation results present that the IBFS is more robust because it models every element with the relevant and up-to-date models. Consequently, the computation time required by the proposed method was checked on four large systems, with high number of modern DGs. The results show that the IBFS solves large distribution system with as many as 5000 buses, 10 loops and 30 different DGs in 74 milliseconds. These results cover the computation of the short-circuit currents of four standard short-circuits, and the whole faulted system state. This extremely low computation time shows that the IBFS is especially useful for real-time calculation sin which the computation time is of crucial importance.

The organization of the remaining part of this paper is: Section II describes the distribution system modeling, Section III outlines the idea behind the proposed SCC method, and Section IV presents the IBFS procedure for computation of the state of the system with short-circuit. The computation results are shown and discussed in Section V, while the concluding remarks are derived in Section VI.

II. Modeling of the Distribution System Elements

In this section the SCC models of distribution system elements are described. Modern DGs are mainly focused.

A. Power Transformers, Lines, and Load Models

Power transformers are modeled as a short-circuit impedance in parallel with a magnetizing admittance [7]. Lines are presented by $\prod$ schemes [7]. These models, have been used for almost a century in the power system analysis, and thus they are not presented in this paper.

A usual trend in distribution system SCCs is neglecting of the influence of loads [1], [2]. A reciprocal comparison of feeder head fault currents, obtained by three different load models: 1) complete neglecting, 2) pre-fault currents, and 3) constant impedances is shown in [17]. It is deduced in [17] that the differences in results obtained by the latter two models are minor. Nonetheless, it is deduced in [18] that complete neglecting of the influence of loads can cause high inaccuracy in calculating feeder head currents. Therefore in this paper, the influence of loads is taken into account as pre-fault currents.

B. The DG Models

DGs are divided into four different types, based on their SCC models [19]:

1) Type 1: synchronous generator directly connected to the grid.

2) Type 2: induction generator directly connected to the grid).

3) Type 3: DFIG.

4) Type 4: IBDG.

Type 1 DG and Type 2 DG are explained in detail in [19]. These models have been successfully used in the power system analysis for the last several decades. Therefore, explanation of these models is omitted in this paper. Their models are presented in Fig. 1 and Fig. 2, respectively.

In Fig. 1, ideal voltage sources for sub-transient, transient and steady-state, are marked with V''_+, V'_+ and V_+, respectively. Positive sequence impedances for sub-transient, transient and steady-state, are marked with Z''_+, Z'_+ and Z_+, respectively. The negative sequence impedance is marked with Z_-.

In Fig. 2, V' is the voltage source behind transient reactance X'. The rotor's resistance and leakage reactance, are marked with R_r and X_r, respectively. The stator's resistance and leakage reactance, are marked with R_s and X_{ls}, respectively. The magnetizing reactance is marked with X_m. The slip is marked with s.

Type 3 DG presents the toughest challenge for modeling, as the DFIG's model for the SCC purposes strongly depends on the intensity of the fault as well as on the protection scheme that is installed in the rotor's power converter. In most cases DFIG possesses the protection device called the crowbar, which, in case of the severe faults, short-circuits the rotor in order to protect the power converter [2], [14]−[16]. In this case, DFIG's model for SCC purposes becomes akin to the Type 2 DG's model [2], [12]−[16]. The only difference between these two models is that in case of the DFIG, the resistance of the crowbar needs to be inserted in series with the stator's resistance (Fig. 2). The value of this resistance is in most cases supplied by the manufacturer of the DFIG, and its value can be more than twenty times higher than the rotor's resistance [12]. Therefore, the crowbar's resistance should not be neglected when the accurate SCC is desired.

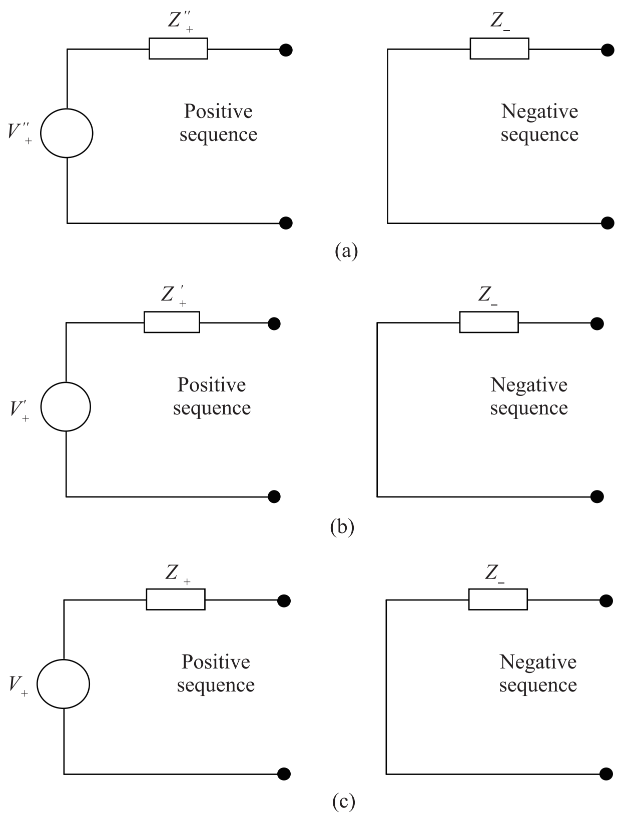

Fig. 1. Synchronous generator models for the SCC purposes. (a) Subtransient state. (b) Transient state. (c) Steady state.

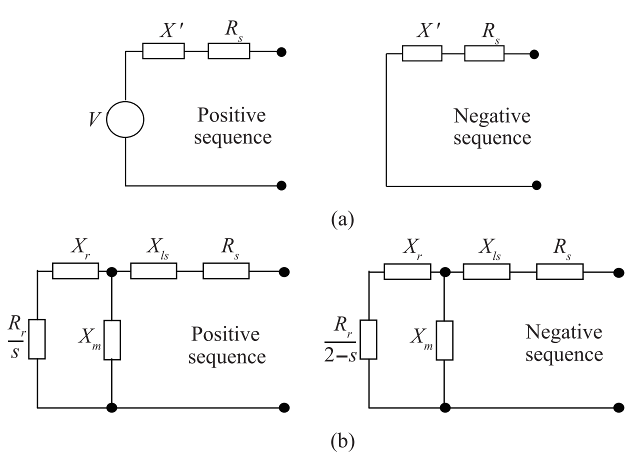

Fig. 2. Induction generator models for the SCC purposes. (a) Transient state. (b) Steady state.

If the short-circuit is not as intense (e.g., in the case that it happens at the location remote from the DFIG) the crowbar will not be activated and the power converter would control the DFIG's injected short-circuit current. Moreover, if a different device for the converter's protection is installed in the DFIG, which would allow the power converter to stay active over the whole duration of the short-circuit, the converter would manage to have control over the fault current through the whole short-circuit period even in the case of severe short-circuits. This device is installed in most of the modern DFIGs and it is called chopper [15], [16].

In the latter two cases, when a DFIG manages to continue to control its short-circuit current, it should be modeled same as the Type 4 DG, explained below [15], [16].

In the work presented in this paper, the intensity of the short-circuit is measured from the voltage at the DFIG's point of common coupling (PCC) at the moment of short-circuit. The assumption is that the crowbar would react in case that the value of the voltage at the DFIG's PCC drops under the predefined threshold value [15]. If the value of this voltage remains over the threshold, the power converter would stay active and would manage to control the short-circuit current. Moreover, if chopper is installed for the power converter's protection, the short-circuit current supplied by DFIG will be controlled also.

Type 4 DG has the same model, no matter what is the original energy source [2], [13]−[16]. A fault current is limited to 1−1.5 time of the rated current in order to protect the power converter [13]−[16]. Controllers inside the power converter are in most cases designed to provide positive sequence symmetrical currents, even in cases of unsymmetrical short-circuits [15], [16]. Therefore, the IBDG model for the SCC purposes is an controlled current source with the positive sequence current [13]−[16]. The controlled current source model is a particular challenge for traditional SCC procedures [1], [2], because these procedures are not designed to cope with generators that are modeled with other than a traditional voltage source behind impedance model. The method proposed in this paper deals with such models with a high effectiveness.

The assumption in this work is that power converters are designed to limit short-circuit currents to the IBDGs' rated currents, with the equal phase angles as the ones of the pre-fault currents [16]. Nonetheless, alike the DFIGs, different manufacturers can use distinct short-circuit current limitations and also distinct phase angles settings. However, if the manufacturer provides data about the control strategy implemented in its IBDG, any value for the fault current of the IBDG could

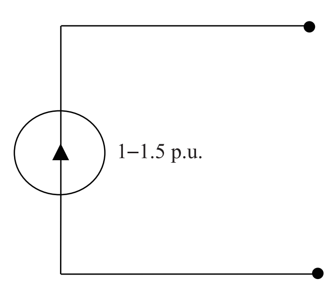

Fig. 3. IBDG model for the SCC purposes.

be integrated in the SCC presented in this work. In Fig. 3 the IBDG model is shown.

C. LVRT Requirements

DGs should make a contribution to distribution system support in not only normal operation but also in the faulted conditions. To comply with that notion, DGs should stay connected to the system in an event of fault and contribute a support to the distribution system if possible. As Types 3 and 4 DGs have controlled current responses, these DG types can stay connected to the system throughout the duration of the fault. The competence to undergo a fault or other disturbances, which cause the voltage change at the PCC, without being disconnected from the system, is called the LVRT capability [20]. Most of the countries have strictly defined grid codes with the LVRT requirements for transmission systems. However some of the modern distribution codes, such as German [21] and Irish [22], have the LVRT requirements for distribution systems also. Other countries will most probably start introducing the LVRT requirements to distribution codes as well. In Fig. 4 the Irish LVRT requirements regarding modern DGs (Types 3 and 4 DGs) are presented. If voltage of any phase at the DG's PCC drops to a value above the borderline (bold line in Fig. 4), the DG must remain connected to the system. From Fig. 4 it is obvious that even if the voltage drops to 15% of the rated voltage, DG must remain connected for the first 625 ms. If the voltage drops below the borderline, DG can be disconnected. Other codes have slightly different threshold values, but the principle is the same.

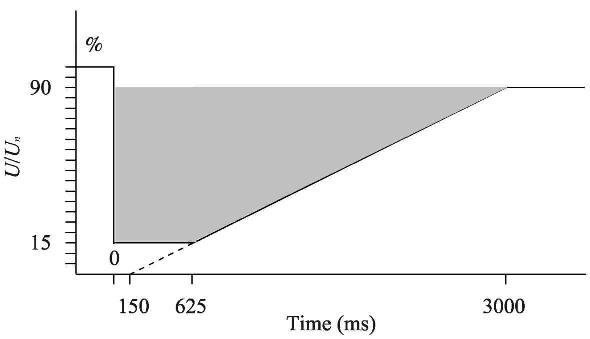

Fig. 4. Irish LVRT requirements for modern DGs [21].

Based on the discussion about DFIG's modeling and the LVRT requirements for DFIGs and IBDGs, in Fig. 5 the algorithm is proposed for deciding which model should be used for DFIGs, and if DFIGs and IBDGs should stay connected to the system throughout the duration of the fault.

D. Distribution System Model-segments

The complete SCC procedure presented in this work is executed in the sequence domain. Thus, the three-phase system with short-circuit is scaled-down to three single-phase systems, in positive, negative and zero sequences. As the system before the short-circuit is assumed to be balanced in the symmetrical state, the three sequence circuits are decoupled at all places aside from the faulted bus (bus k). In accordance with the distribution system element models presented in previous subsections, the sequence circuits could be formed by Γ segments, presented in Fig. 6. In Fig. 6, with L and l are marked sending and receiving nodes, respectively; with $\hat{z}_l$ and $\hat{y}_{lo}$ are marked series and shunt parameters of these segments, respectively, while with $\hat{I}_l$ and $\hat{I}_{lo}$ are marked their currents; $\hat{U}_L$ and $\hat{U}_l$ are the voltages of the sending and receiving nodes of these segments, P_l is the load, $\hat{I}_{lP}$ is its current, DG_l is the mark for DG, while $\hat{I}_{DGl}$ is the DG's current. G denotes the ground.

III. Four Key Decompositions of the State of the System With Short-circuit

In this paper, SCC is executed through four decompositions of the state of the system with short-circuit [7], [8], [17] (Fig. 7). The DC state is not discussed in this work. As the state of the system before the short-circuit (pre-fault state) is known, SCC is scaled-down to the computation of the Δ-circuit. The state of the system with short-circuit is computed by the superposition of the Δ-circuit state and the known state of the system before the short-circuit [7]. The state of the system before the short-circuit is known either from the load flow simulation [6] or from the real-time state estimation [19].

It is important to consider that the short-circuit currents injected by all DGs consist of superposition of their pre-fault currents and their Δ-circuit currents. The (sub-transient, transient or steady-state) impedances of DGs remained in the Δ-circuit model, and hence their currents in the Δ-circuit are calculated by considering these impedances. Just the short-circuit currents injected by IBDGs are obtained completely from the state of the system before the short-circuit, because the assumption is that the power converters are set to supply the rated currents through the entire short-circuit period. Nonetheless, in the case that the power converter is set to inject the current that has a greater value than the pre-fault current, the difference between these two currents would need to be added in corresponding buses of the Δ-circuit. However, this is beyond the scope of this paper.

In this paper, four usual short-circuits are studied: single line to ground (SLG), double line to ground (2LG), double line (2L) and three line (to ground) (3LG). The Δ-circuit short-circuit currents in the sequence domain, at the fault location (bus k), are computed with the well-known formulae, as shown in Table II, in accordance with [7], [9].

TABLE II
FORMULAE FOR COMPUTATION OF FAULT CURRENTS AT THE SHORT-CIRCUIT LOCATION

	SLG (phase a)	2LG (phases b, c)	2L (phases b, c)	3LG
$\hat{J}_k^{\Delta +}$	$\frac{\hat{U}_{ka}}{\hat{Z}_k^+ + \hat{Z}_k^- + \hat{Z}_k^0}$	$\frac{(\hat{Z}_k^- + \hat{Z}_k^0)\hat{U}_{ka}}{\hat{Z}_k^+\hat{Z}_k^- + \hat{Z}_k^+\hat{Z}_k^0 + \hat{Z}_k^-\hat{Z}_k^0}$	$\frac{\hat{U}_{ka}}{\hat{Z}_k^+ + \hat{Z}_k^-}$	$\frac{\hat{U}_{ka}}{\hat{Z}_k^+}$
$\hat{J}_k^{\Delta -}$	$\frac{\hat{U}_{ka}}{\hat{Z}_k^+ + \hat{Z}_k^- + \hat{Z}_k^0}$	$\frac{-\hat{Z}_k^0\hat{U}_{ka}}{\hat{Z}_k^+\hat{Z}_k^- + \hat{Z}_k^+\hat{Z}_k^0 + \hat{Z}_k^-\hat{Z}_k^0}$	$-\frac{\hat{U}_{ka}}{\hat{Z}_k^+ + \hat{Z}_k^-}$	0
$\hat{J}_k^{\Delta o}$	$\frac{\hat{U}_{ka}}{\hat{Z}_k^+ + \hat{Z}_k^- + \hat{Z}_k^0}$	$\frac{(\hat{Z}_k^- + \hat{Z}_k^0)\hat{U}_{ka}}{\hat{Z}_k^+\hat{Z}_k^- + \hat{Z}_k^+\hat{Z}_k^0 + \hat{Z}_k^-\hat{Z}_k^0}$	0	0

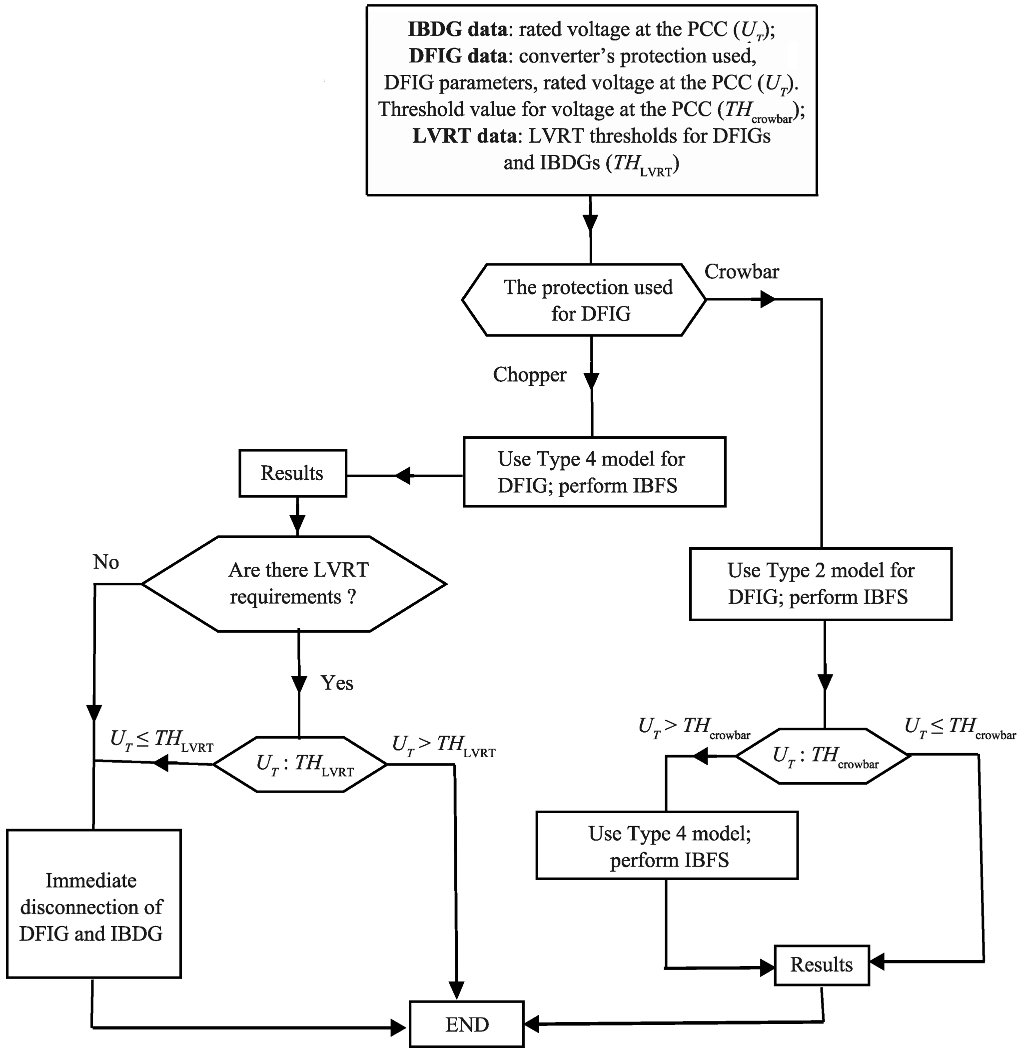

Fig. 5. Algorithm for determination of DFIG's model and the LVRT requirements.

$\hat{Z}_k^+$, $\hat{Z}_k^-$, $\hat{Z}_k^0$ are Thévenin impedances seen from the bus with short-circuit, in the positive, negative and zero sequences, respectively. $\hat{U}_{ka}$ is the (known) phase of voltage at the bus with short-circuit, in the state of the system before the short-circuit.

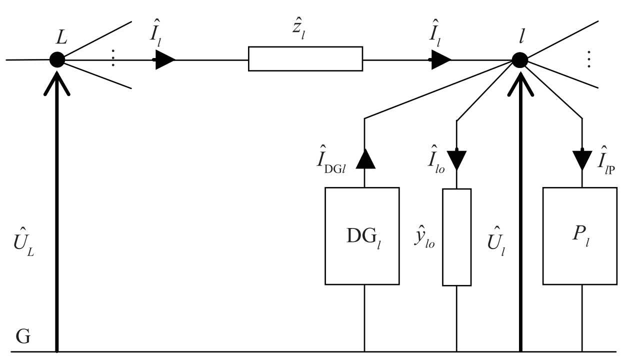

Fig. 6. Γ segment.

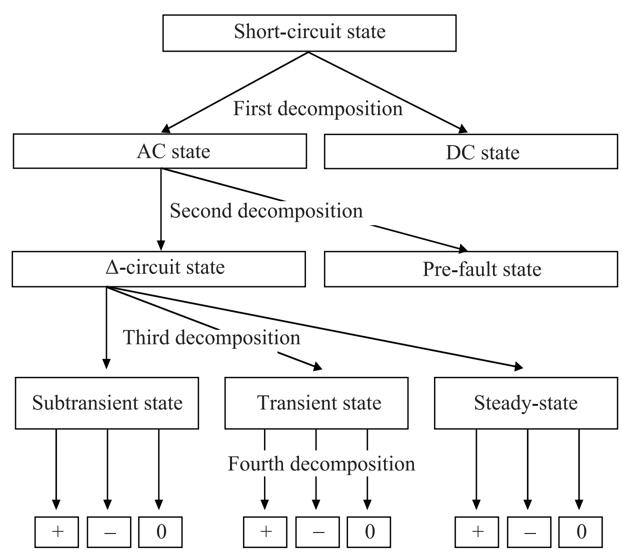

Fig. 7. Decompositions of the state of the system with short-circuit.

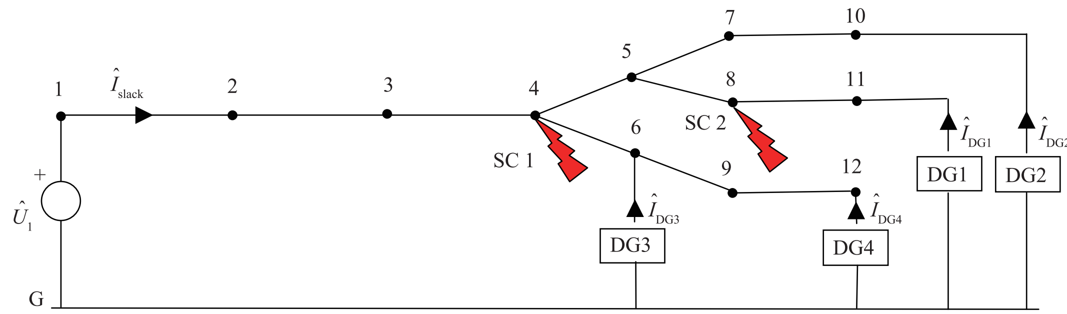

Fig. 8. The 12-bus distribution system.

IV. THE Δ-CIRCUIT STATE COMPUTATION–THE IBFS PROCEDURE

The computation of the faulted system state is scaled-down to the computation of the Δ-circuit state. The Δ-circuit state is computed with the IBFS procedure. The traditional method for the loop compensation has an inner iterative procedure inside the main (also iterative) procedure [3], [20]. In the work presented in this paper, this inner procedure is avoided. In the IBFS procedure presented in this paper, the actual mismatches of breakpoint voltages obtained in every iteration using (2), are used for the calculation of the next iteration of the breakpoint currents using (3) and (4). The proposed IBFS procedure for computation of the whole Δ-circuit state is as shown in (1)−(6):

Backward sweep:

$$(\hat{I}_l^{\Delta s})^{h+1} = \hat{J}_l^{\Delta s} + (\hat{J}_{ci}^{\Delta s})^h + \hat{y}_{lo}^s(\hat{U}_l^{\Delta s})^h + \sum_{j\in\alpha_l}(\hat{I}_j^{\Delta s})^{h+1}$$
$$l = n+p,\ldots,3,\,2,\,1;\quad s=+,-,0. \tag{1}$$

Forward sweep:

$$\left(\hat{U}_l^{\Delta s}\right)^{h+1} = \left(\hat{U}_L^{\Delta s}\right)^{h+1} - \hat{z}_l^s\left(\hat{I}_l^{\Delta s}\right)^{h+1}$$
$$l=\ 2,\ 3,\ \ldots\ ,n+p;\quad s=+,\,-,\,0. \tag{2}$$

Breakpoint currents correction:

$$(\Delta\hat{J}_c^{\Delta s})^h = \hat{Y}_N^s\left[(\hat{U}_1^{\Delta s})^{h+1} - (\hat{U}_2^{\Delta s})^{h+1}\right]$$
$$\hat{Y}_N^s = \left(\hat{Z}_T^s\right)^{-1},\quad s=+,\,-,\,0. \tag{3}$$

$$(\hat{J}_c^{\Delta s})^{h+1} = (\hat{J}_c^{\Delta s})^h + (\Delta\hat{J}_c^{\Delta s})^h,\quad s=+,-,0. \tag{4}$$

The short-circuit currents are known from Table II:

$$\hat{J}_l^{\Delta s} = \begin{cases} 0, & l\neq k \\ \hat{J}_k^{\Delta s}\neq 0, & l=k \end{cases},\quad s=\ +,\ -,\ 0. \tag{5}$$

h corresponds to the number of the actual iterations; Δ in the superscript corresponds to the Δ-circuit; n refers to the number of buses in the distribution system of interest; p refers to the number of loops; $\hat{z}_l^s$ and $\hat{y}_{lo}^s$ are the series and shunt parameters of the lth Γ segment in the sequence domain; α_l is the set of Γ segments which are successors of segment l; $\hat{U}_L^{\Delta s}$ and $\hat{U}_l^{\Delta s}$ are the sequence domain voltages; $\hat{I}_l^{\Delta s}$ is the current of lth Γ segment; $\hat{J}_{ci}^{\Delta s}$ is the breakpoint current in the case that the node l is the breakpoint node; $\hat{J}_l^{\Delta s}$ are grouped in the vector $\hat{J}_c^{\Delta s}$; $\Delta\hat{J}_c^{\Delta s}$ are corrections of breakpoint currents [20]; $(\hat{U}_1^{\Delta s})^{h+1}$ and $(\hat{U}_2^{\Delta s})^{h+1}$ are the $(h+1)$th approximations of vectors of the first and second breakpoint nodes and their dimensions are $p\times 1$. $(\hat{U}_1^{\Delta s})^{h+1} - (\hat{U}_2^{\Delta s})^{h+1}$ is the vector of breakpoints voltage mismatches; $\hat{Y}_N^s$ and $\hat{Z}_T^s$ are Norton and Thévenin matrices seen from the breakpoints, in the sequence domain, and their dimensions are $(p\times p)$ [5], [23]. $(\hat{J}_c^{\Delta s})^h$ is the vector of actual approximations of breakpoint currents in the sequence domain, $(\Delta\hat{J}_c^{\Delta s})^h$ refers to the vector of corrections of the hth approximations of breakpoint currents in the sequence domain; $(\hat{J}_c^{\Delta s})^{h+1}$ refers to the vector of $(h+1)$th approximations of breakpoint currents in the sequence domain, and their dimensions are $p\times 1$. Voltages of the supply point in the Δ-circuit are zero: $\hat{U}_1^{\Delta s}=0$, $s=+,-,0$. Initial approximations of voltages of all buses and initial approximations of breakpoint currents in the Δ-circuit are zero.

The calculation procedure is terminated after it converges according to (6):

$$\left|(\hat{U}_l^{\Delta s})^{h+1} - (\hat{U}_l^{\Delta s})^h\right| \leq \varepsilon_U,\quad l=\ 2,\ 3,\ \ldots\ ,n+p. \tag{6}$$

V. COMPUTATION RESULTS AND THEIR DISCUSSION

The number of three-phase buses in the distribution systems tested by the IBFS procedure is in the range from 12 to 5000. First, the test results are shown for a 12-bus distribution system depicted in Fig. 8. The supply point of the system is the bus 1. It has the stated three-phase symmetrical voltage (phase voltage equal to: $U_1 = (21/\sqrt{3})$ KV). All lines are with equal parameters, shown in Table III. The maximal current of these lines is: $I_{\max} = 400$ A. As the positive and negative parameters have reciprocally identical values, the negative sequence parameters have not been presented in Table III. All four DG types are connected to the system. DG1, DG2, DG3 and DG4 (Fig. 8) correspond to Type 1, Type 2, Type 3 and Type 4 DGs, respectively. DG parameters are same as in [2]. DG1, DG2, DG3 and DG4 supply the same power in the pre-fault conditions. Every DG injects six percent of the total required power,which means that the total power injected by four DGs is nearly twenty five percent of the total load. All loads are of equal powers.

In order to validate the applicability and effectiveness of the proposed method, the IBFS is compared with the EVS [1]. Because EVS is not designed to deal with DFIGs and IBDGs, this example is performed with DG3 and DG4 detached from the test system. Moreover, as the EVS does not take into account loads, their influence has also been neglected in the IBFS for this example. Therefore, the proposed IBFS method is reduced to match the EVS completely. In Table IV the computation results of this example are presented. The results are presented for the case that the bus 4 is the faulted bus (SC1), for the magnitudes of the following currents: I_{slack} (supplied by the HV/MV substation), I_{DG1} (supplied by DG1), I_{DG2} (supplied by DG2) and I_{fault} (the short-circuit current at the faulted bus). Results are shown for two marginal cases (the lowest and the highest short-circuit currents): SLG (phase a) and 3LG.

TABLE III
SECTION PARAMETERS OF THE TEST SYSTEM

R_+ (Ω/mile)	X_+ (Ω/mile)	B_+ (μs/mile)	R_o (Ω/mile)	X_o (Ω/mile)	B_o (μs/mile)
0.26	0.23	1.88	0.77	0.67	0.63

TABLE IV
COMPARISON OF COMPUTATION RESULTS OBTAINED BY ABRIDGED IBFS AND EVS METHODS FOR SCC

	IBFS (A)	EVS (A)	Difference (%)
I_{slack} (SLG)	4348.73	4418.87	1.6
I_{slack} (3LG)	7651.19	7648.33	0.04
I_{DG1} (SLG)	224.83	182.05	18.7
I_{DG1} (3LG)	462.16	407.65	11.9
I_{DG2} (SLG)	276.48	235.22	14.8
I_{DG2} (3LG)	604.32	562.77	6.9
I_{fault} (SLG)	4850.04	4846.14	0.1
I_{fault} (3SLG)	8717.67	8618.75	1.2

It is suggested in [17], [18] that neglecting loads leads to errors when calculating currents on the feeder head (where the protection equipment is usually installed). According to [17], the highest error is noticed for the SLG. Therefore, current I_{slack} is further compared when calculated by IBFS with loads taken into account and EVS (where loads are neglected). SLG is simulated at bus 8 (SC2). The neglecting of loads in EVS is partially compensated by multiplying the pre-fault voltage at the fault location by coefficients with values from 1.05 to 1.10. Similar coefficients are used for the DG's pre-fault currents. According to [17], with an increase in distance between short-circuit and the supply point, the percentage of error made by neglecting loads increases as well. Fig. 9 presents percentage differences (DI (%)) in magnitudes of current I_{slack} is calculated by both methods, for different distances from the supply point to the fault location. Distance is marked with L. To simulate faults near to the supply point as well as those that are far from the supply point, the distance L was increased from 5 km to 25 km, in four equal steps.

Afterwards, the proposed method was tested on the distribution system from Fig. 8 but with all four DGs attached to the system. The influence of loads was also considered for this example. Faults were simulated in buses 4 (SC1) and 8 (SC2). Four standard faults were tested: 3LG, 2L (phases b and c), 2LG (phases b and c), and SLG (phase a). Computation results are presented in Table V and Table VI, for SC1 and SC2, respectively.

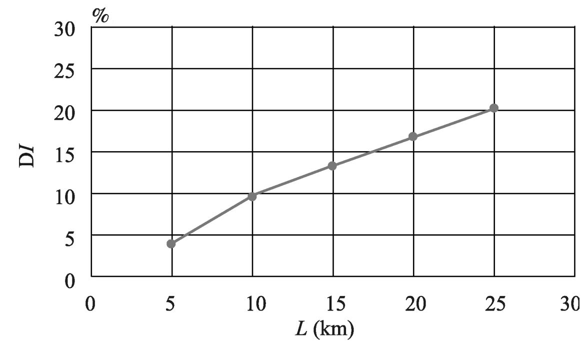

Fig. 9. Differences of the feeder head current calculated with loads taken into account (IBFS) and loads neglected (EVS).

TABLE V
COMPUTATION RESULTS FOR SC1

	I_{DG1}(A)	I_{DG2}(A)	I_{DG3}(A)	I_{DG4}(A)	I_{slack}(A)	I_{fault}(A)
3LG	475	621	609	156	7763	9664
2L	399	556	539	156	6685	8416
2LG	404	559	523	156	6877	8614
SLG	223	274	258	156	4246	5227

TABLE VI
COMPUTATION RESULTS FOR SC2

	I_{DG1}(A)	I_{DG2}(A)	I_{DG3}(A)	I_{DG4}(A)	I_{slack}(A)	I_{fault}(A)
3LG	499	524	118	156	4405	5702
2L	419	468	118	156	3771	4932
2LG	424	471	118	156	3855	5024
SLG	226	238	118	156	2371	3109

In the case of SC1, the short-circuit is near to DG3. Therefore SC1 is dangerous enough to cause the activation of the crowbar. It is also severe regarding LVRT threshold (which is assumed 15 % of the rated voltage, in accordance with the Irish Distribution Code). Thus, it needs to be disconnected from the system. Therefore, after the disconnection, DG3's fault current contribution will be zero. Nonetheless, the short-circuit SC2 is located remote from DG3, and therefore the voltage at the DG's PCC remains over the crowbar's and LVRT's threshold values. Hence, converter maintains its control over the fault current and DG3 should stay connected to the grid. It is important to consider that in accordance with the algorithm proposed in this work (Fig. 5), in the case of SC2, two IBFS procedures need to be executed.

Lastly, the proposed IBFS method was performed on four large-scale distribution systems (*A*, *B*, *C* and *D*). The number of buses in these test systems is in range from 500 to 5000, the number of loops from 0 to 10, while the number of DGs is in range from 4 to 30. The computation times (in milliseconds) required for SCC of these test systems by the IBFS method, are presented in Table VII. Computation time includes the time needed for execution of a single load flow computation of the system's state before the short-circuit, and time required for computation of four metal short-circuits, along with computation of the entire state of the system with short-circuit. Load Flow is computed by the same IBFS method [6], with loads and DGs modeled as constant powers.

All tests have been performed on a PC, Intel i3−2330 M, 4 GB RAM. All computation procedures have been coded in FORTRAN 2008.

TABLE VII
EXECUTION TIMES REQUIRED FOR SCCS OF FOUR DISTRIBUTION SYSTEMS WITH LARGE NUMBER OF BUSES

Test system	Number of buses	Number of loops	Number of DG	Execution time (ms)
A	500	0	4	6.12
B	1250	4	10	19.06
C	2500	6	20	39.73
D	5000	10	30	74.92

The following facts can be concluded from the research presented in this work:

1) It is obvious from Table IV that when the influence of loads is not taken into account in the IBFS, the computation results for the fault current at the short-circuit location are almost mutually equal when computed by IBFS and EVS. The similar is valid for results for the current injected by the HV/MV substation, for which the differences do not exceed 2 %. Nonetheless, rather high differences (up to 19 %) are observed for currents injected by Type 1 and Type 2 DGs. It is a consequence of the EVS's neglecting of the DGs' currents of the state of the system before the short-circuit. Therefore, besides the fact that EVS is not meant to deal with DFIGs and IBDGs, this method introduces rather high errors in the computation results for currents injected by synchronous and induction DGs. This error is avoided in the proposed IBFS method.

2) Fig. 9 shows that by neglecting loads, EVS creates a rather high error in calculating the feeder head current. The error is close to 20 % if the short-circuit happened 25 km from the supply point. This error could seriously affect the settings and coordination of the distribution system's protection equipment. As the IBFS takes the influence of loads into account, this error is omitted in the IBFS.

3) From the results presented in Tables V and VI it can be concluded that the up stream grid (transmission system) compounds the highest short-circuit current, whereas the least short-circuit current contribution is from the IBDG (Type 4 DG). In regard to DGs, the highest short-circuit current contributions are from types 1 and 2 DGs (and Type 3 DG, in a case that the crowbar reacted). This matches well with the recent literature [2], [14]−[16]. However, rather interesting results are obtained for the short-circuit current contribution of the DFIG (Type 3 DG). The results for the DFIG's short-circuit current could be significantly different depending on if the crowbar reacted. In the case that crowbar reacted, DFIG's short-circuit current was almost six times higher than in the case that crowbar has not reacted. Thus, the short-circuit current contribution of the DFIG should be modeled extremely carefully. The classical assumption from traditional SCCs, that crowbar will always react [2] could introduce unacceptable errors in cases of the faults located remote from the DFIG. This computation error could cause the disconnection of the DFIG because of the false assumption of much larger current, and in that way directly affect the LVRT requirements for DFIG to stay connected and support the system. Therefore, the block-diagram presented in Fig. 5 could be highly practical for this purpose.

4) Lastly, results from Table VII show that the proposed IBFS method solves a huge distribution system which consists of 5000 buses, 10 loops and 30 different DGs in 74.92 milliseconds. This result shows that the IBFS method is particularly effective for SCCs of modern, large-scale weakly-meshed distribution systems, with a high penetration of DGs.

VI. CONCLUDING REMARKS

In the work presented in this paper, an extremely robust and efficient SCC method (IBFS) suitable for active, large-scale weakly-meshed distribution systems is proposed. The IBFS method deals with loops with the highest efficiency, by avoiding the traditional iterative procedure for the loop compensation inside the main procedure. Additionally, the short-circuit current contribution of the modern DGs is taken into account with a high efficiency.

The LVRT requirements are considered and incorporated in the proposed procedure. This is highly important as in recent years, increasing number of countries is introducing the LVRT requirements to their distribution codes, and therefore all modern DGs must comply with them. Hence, SCC procedure for modern distribution system must consider the LVRT requirements.

The accuracy and robustness of the proposed IBFS method make it highly effective for the construction of many other DMS calculations, such as: settings and coordination of the relay protection, checking of the distribution system equipment overstressing, selection of protection equipment, etc.

Lastly, a particularly low calculation time for the SCCs of large-scale distribution systems makes the IBFS suitable in many segments of the distribution system management.

REFERENCES

[1] *Short-circuit Currents in Three—-Phase a.c. Systems-Part 0: Calculation of Currents*, IEC International Standard 60909-0, 2001.

[2] T. N. Boutsika and S. A. Papathanassiou, "Short circuit calculations in networks with distributed generation," *Electr. Power Syst. Res.*, vol. 78, no. 7, pp. 1181−1191, Jul. 2008.

[3] X. F. Zhang, F. Soudi, D. Shirmohammadi, and C. S. Cheng, "A distribution short circuit analysis approach using hybrid compensation method, *IEEE Trans. Power Syst.*, vol. 10, no. 4, pp. 2053−2059, Nov. 1995.

[4] W. M. Lin and T. C. Ou, "Unbalanced distribution network fault analysis with hybrid compensation," *IET Gen. Transm. Distrib.*, vol. 5, no. 1, pp. 92−100, Jan. 2011.

[5] R. A. Jabr and I. Džafić, "A fortescue approach for real-time short circuit computation in multiphase distribution networks," *IEEE Trans. Power Syst.*, vol. 30, no. 6, pp. 3276−3285, Nov. 2015.

[6] V. C. Strezoski and P. M. Vidović, "Power flow for general mixed distribution networks," *Int. Trans. Electr. Energy Syst.*, vol. 25, no. 10, pp. 2455−2471, Oct. 2015.

[7] A. R. Bergen and V. Vittal, "*Power Systems Analysis*," 2nd ed. New Jersey, USA: Prentice Hall, 2000.

[8] P. M. Anderson, "*Analysis of Faulted Power Systems*," New York, NY, USA: IEEE Press, 1995.

[9] M. Abdel-Akher and K. M. Nor, "Fault analysis of multiphase distribution systems using symmetrical components," *IEEE Trans. Power Del.*, vol. 25, no. 4, pp. 2931−2939, Oct. 2010.

[10] V. Gevorgian, M. Singh, and E. Muljadi, "Symmetrical and unsymmetrical fault currents of a wind power plant," in *Proc. 2012 IEEE Power and Energy Society General Meeting*, San Diego, CA, USA, 2012, pp. 1−8.

[11] R. A. Walling and M. L. Reichard, "Short circuit behavior of wind turbine generators," in *Proc. 2009 62th IEEE Ann. Conf. Protective Relay Engineers*, Austin, TX, USA, 2009, pp. 492−502.

[12] M. Fischer and Â. Mendonca, "Representation of variable speed full conversion wind energy converters for steady state short-circuit calculations," in *Proc. 2012 IEEE PES Transmission and Distribution Conference and Exposition*, Orlando, FL, USA, 2012, pp. 1−7.

[13] D. F. Howard, T. M. Smith, M. Starke, and R. G. Harley, "Short circuit analysis of induction machines-wind power application," in *Proc. 2012 IEEE PES Transmission and Distribution Conference and Exposition*, Orlando, FL, USA, 2012, pp. 1−8.

[14] D. F. Howard, "Short-circuit currents in wind-turbine generator networks," Ph.D. dissertation, Georgia Institute of Technology, Atlanta, GA, USA, 2013.

[15] J. R. Williams and B. Karlson, "Wind power plant short-circuit modeling guide," Sandia National Laboratories, Albuquerque, NM, USA, SAND 2012-6664, Aug. 2012.

[16] Joint Working Group, "Fault current contribution from wind plants," *Proc. 68th Ann. Conf. Protective Relay Engineers*, 2015, pp. 137−227.

[17] L. Strezoski and M. Prica, "The influence of load modeling on distribution protective relay current," in *GEARED Student Workshop*, Charlotte, NC, USA, 2015.

[18] A. Tan, W. H. E. Liu, and D. Shirmohammadi, "Transformer and load modeling in short circuit analysis for distribution systems," *IEEE Trans. Power Syst.*, vol. 12, no. 3, pp. 1315−1322, Aug. 1997.

[19] L. V. Strezoski and M. D. Prica, "Real-time short-circuit analysis of active distribution systems," *Proc. 2016 IEEE Power and Energy Conference at Illinois (PECI)*, Urbana, IL, USA, 2016, pp. 1−8.

[20] D. Van Tu, S. Chaitusaney, and A. Yokoyama, "Maximum-allowable distributed generation considering fault ride-through requirement and reach reduction of utility relay," *IEEE Trans. Power Del.*, vol. 29, no. 2, pp. 534−541, Apr. 2014.

[21] Distribution system operators-ESB networks, Irish Distribution Code, 2015.

[22] Bundesverband der Energie-und Wasserwirtschaft e.V., Guideline for generating plants connection to and parallel operation with the medium-voltage network, 2008.

[23] D. Shirmohammadi, H. W. Hong, A. Semlyen, and G. X. Luo, "A compensation-based power flow method for weakly meshed distribution and transmission networks," *IEEE Trans. Power Syst.*, vol. 3, no. 2, pp. 753−762, May 1988.

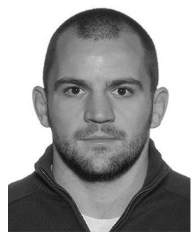

Luka V. Strezoski (S' 2013) received the B.S. and M. Sc. degrees in power engineering from the University of Novi Sad in 2013 and 2014, respectively. He is working toward the Ph.D. degree. He is currently with the Electrical Engineering and Computer Science Department, Case Western Reserve University, Cleveland, OH, USA, as a research scholar. His research interests include distribution system modeling, power flow and short-circuit calculations, and integration of distribution generators to the DMS power applications. Corresponding author of this paper.

Marija D. Prica (M' 2010) received the B.S. and M.S. degrees in power engineering from the University of Novi Sad in 2000 and 2006, respectively, and Ph.D. degree from Carnegie Mellon University, Pittsburgh, PA in 2010. She is an assistant professor at Case Western Reserve University, Cleveland, OH. Her research interests include distribution system planning and protection, integration of advanced technologies and control, decision-making for future electricity systems, and optimization of energy storage operation.